THE JOURNAL OF PHYSICAL CHEMISTRY C

Article

Cite This: J. Phys. Chem. C 2018, 122, 19146−19152

pubs.acs.org/JPCC

Nonlinear Polarization and Low-Dissipation Ultrafast Optical Switching in Phosphorene

Ravindra Shinde* and Abhishek Kumar Singh*

Materials Research Center, Indian Institute of Science, Bangalore 560012, India

Supporting Information

ABSTRACT: Fundamental limits to the computation using silicon-based devices stimulate other emerging and viable alternatives. Manipulation of the electrical and optical properties with the ultrafast and intense electric fields offers one of such alternatives. Here, we study the interaction of high-intensity pulsed femtosecond laser of various intensities and carrier frequencies with a monolayer phosphorene using the real-time real-space time-dependent density functional theory. The nonlinear induced currents are entirely reversible but are phase-shifted compared to low-intensity lights within the period of incident laser. We observe optical Kerr effect associating the changes in the number of free charge carriers with the change in the refractive index of the material, which subsequently characterizes the material's ability of dielectric switching. The transient changes in refractive index are reversible up to a certain threshold, suggesting that the properties can be switched on the timescale of an optical period, enabling the possibility of operating solid-state electronic devices at optical frequencies. The amount of irreversibly transferred energy into the system is found to be much smaller than that of the state-of-the-art metal−oxide field-effect transistor, thereby making phosphorene a promising candidate for high-speed electronics.

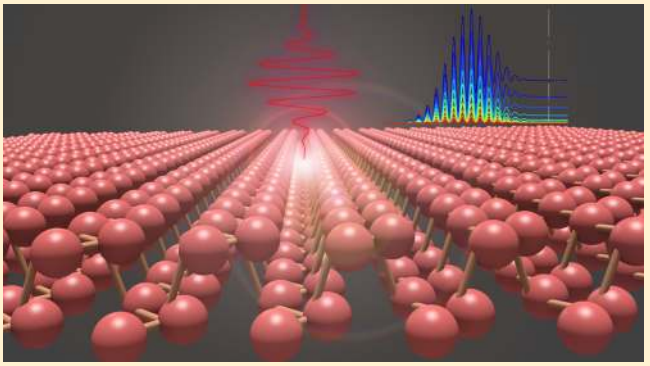

INTRODUCTION

Computing has become an indispensable tool of our lives. The escalating complexity of tasks has led to the ever-increasing demand for faster computation. This has resulted in a steady progress in the transistor integration technologies. The nanoscale lithography technique today allows several million transistors per square millimeter.[1] However, there are fundamental limits to the computation, such as, Abbe diffraction, interconnect capacitance, and heat dissipation, which affect its speed.[2] An altogether new approach of computation is necessary to circumvent these limits. Computation based on the photo-induced phenomenon, such as manipulation of electronic and optical properties at the nanoscale, can offer an alternative to the conventional silicon-based electronics. The two-dimensional (2D) nanoscale materials are the promising and emerging candidates, which exhibit fascinating properties.

Two-dimensional (2D) materials have been at the forefront of the active research in material science because of their extraordinary properties and vast potential for technological applications. After the discovery of graphene,[3,4] several other 2D materials such as transition metal dichalcogenides (TMD) and elemental quasi-2D sheets such as silicene,[5] germanene,[6] stanene,[7] and phosphorene[8] were synthesized. Phosphorene, a stable 2D material and an allotrope of black phosphorus, shows interesting properties such as high carrier mobility (10^4 cm^2 V^{-1} s^{-1}),[9] ferroelasticity,[10] non-trivial topology under strain,[11] and layer-dependent direct band gap.[12−14] The monolayer has a direct band gap of 1.5 eV, and it varies with the number of stacked layers, with optical absorption ranging from the infrared to visible region. This high carrier mobility material can also be used as a field effect transistor with a high on/off ratio, suggesting applications in nanoelectronics.[15] Because the direct band gap of phosphorene falls in the mid-range of graphene and TMDs, it is suitable for semiconducting and optoelectronic device applications in the infrared and mid-infrared part of the spectrum. Phosphorene also exhibits interesting anisotropic nonlinear optical properties such as higher harmonic generation (HHG) and has been used as a saturable absorber and optical modulator.[16−22] The nonlinearity of optics is manifested by changes in the optical properties of the materials under the influence of increased intensities of applied light fields. Several interesting nonlinear phenomena such as HHG, above-threshold ionization, and multiphoton absorption are exhibited by materials under the influence of intense laser fields.[23] Materials with such optical nonlinearity find applications in optical communications and optical computing systems.

The speed at which the information or signal can be processed crucially depends on the frequency of electric

Received: May 1, 2018
Revised: July 26, 2018
Published: August 2, 2018

DOI: 10.1021/acs.jpcc.8b04134
J. Phys. Chem. C 2018, 122, 19146−19152

currents induced in that material. Therefore, it is imperative that to increase the signal processing speed, the induced currents should have very high frequencies. Such currents in a material can be induced using high-intensity laser pulses of ultrashort time durations. Several bulk materials such as crystalline silicon, carbon chains, diamonds, CaB_6, and so forth were investigated for these peculiar nonlinear optical properties.[24−29] In the crystalline silicon and quartz, it was shown that these materials could be transformed into highly conducting metals for a very short time because of induced currents.[24,25,30−32] For example, Schiffrin et al. demonstrated that the ac conductivity of fused silica reversibly increases by 18 orders of magnitude within 1 fs.[33] The attosecond dynamics in silica reveals that it can be used as an alternative material for fast switching electronics.[33−35] A laser shape-dependent electron excitation in CaB_6 was studied by Jiao et al.[26] A linear carbon chain with odd and even number of atoms show different trends in induced currents with the application of femtosecond laser.[28] In 2D materials, such as phosphorene and MoS_2, the laser-induced electron dynamics and ultrafast photonics has been studied.[36,37] Phosphorene shows remarkable nonlinear saturable absorption useful in the generation of ultrashort pulses mainly because of high nonlinear refractive index.[16−22] Recently, the possibility of using phosphorene as ultrafast optical switches have been discussed. Uddin et al. found that after depositing phosphorene layer on the optically active medium, phosphorene can switch optical signals with modulation frequencies up to 20 GHz.[17] While Su et al. computed the transient optical absorption of phosphorene under the influence of femtosecond lasers.[38] The switching speed depends on the time taken to switch on and off the induced photocurrent. The necessary criteria for achieving these ultrafast transitions require less dissipation of energy in the material per unit cycle of switching, which is indirectly related to the time-derivative of nonlinear instantaneous dipole moments in the material. However, calculating the nonlinear optical response of a material to intense laser fields is computationally demanding.

For low-intensity lights, the response of a material to the applied electromagnetic field is linear, characterized by linear susceptibilities. However, this linear relationship does not hold good for electromagnetic fields with very high intensities (or typical electric fields of few V per Å).[39,40] For such high intensities, perturbative treatment becomes inadequate because susceptibilities themselves become intensity-dependent, and the time-dependent charge density cannot simply be Taylor-expanded at the ground state value. Several schemes such as Floquet theory, classical trajectories, dressed states, and direct numerical integration of time-dependent dressed Schrödinger equation have been developed to model the nonperturbative regime.[24,25,41] For the first principles description of such interactions of electromagnetic fields with the material, the Schrödinger equation with additional vector potential term needs to be solved. The theoretical treatment involves computation of microscopic field-induced current and the nonlinear polarization P_{NL} in the system.

The manipulation of electronic and optical properties of a given material crucially depends on the microscopic nonlinear polarization P_{NL}. The amount of energy transferred from the incident laser to the material per unit volume can be expressed as

$$W(t) = \int_{-\infty}^{t} E(t')\frac{\mathrm{d}}{\mathrm{d}t'}P_{NL}(t')\mathrm{d}t' \quad (1)$$

This quantity, also known as dissipation, is one of the major limitations to the speed of state-of-the-art electronics, as this cannot be reduced beyond a certain value. For example, the power consumption in a complementary metal−oxide−semiconductor (CMOS) circuit is given by[42]

$$P_{dyn} = C_l V_{dd}^2 f_{0\to 1} \quad (2)$$

where $f_{0\to 1}$ denotes the frequency of energy-consuming transitions, V_{dd} is drain voltage, and C_l is gate capacitance. Hence, the power dissipation is directly proportional to the switching frequency. If the dissipation is reduced, the frequency can be increased by the same factor.

There are two components of the energy transferred to the material: W_{rev} and W_{irrev}, which relate to the reversible and irreversible energy exchange between the electromagnetic field and the material per unit volume, respectively. In ideal situations, the ratio of W_{rev} to W_{irrev} should be as large as possible for an efficient signal processing. This demands a microscopic insight into the light−matter energy exchange at optical frequencies and access to the $W(t)$ on electronic timescales.

Here, we present the effect of the application of ultrafast and intense femtosecond laser to phosphorene (cf. Figure 1),

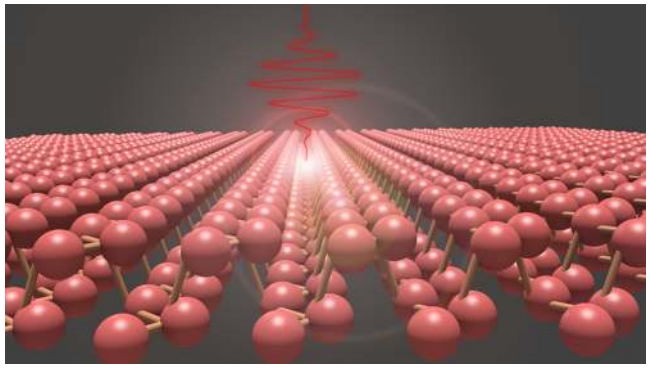

Figure 1. Schematic illustration of the laser−matter interaction. Laser fields of linear polarization and two different carrier frequencies have been used to study nonlinear electron dynamics in the phosphorene.

leading to an interesting optical switching phenomenon for faster electronics, using time-dependent density functional theory (TDDFT). We observe changes in the properties of phosphorene (such as in the number of excited valence electrons, dielectric constant, and amount of irreversible energy pumped in) at the sub-femtosecond timescales and relate them to its ability to be used as a dielectric switch. We show that under various conditions phosphorene can exhibit superior switching with very less dissipation of energy.

THEORETICAL METHODS

TDDFT has become an indispensable, state-of-the-art approach for describing time-dependent phenomenon on the electronic timescales. We used TDDFT for the simulation of electron dynamics under the external time-varying intense laser field. For an N-electron system, a set of Kohn−Sham orbitals $\psi_{i\sigma}(\vec{r},t)$ satisfy the following time-dependent Kohn−Sham equation

DOI: 10.1021/acs.jpcc.8b04134
J. Phys. Chem. C 2018, 122, 19146−19152

$$i\hbar\frac{\partial}{\partial t}\psi_{i\sigma}(\vec{r},t) = H_{ks}(\vec{r},t)\psi_{i\sigma}(\vec{r},t) \quad (3)$$

where $H_{ks}(\vec{r},t)$ is the TDKS Hamiltonian with the following form

$$H_{ks}(\vec{r},t) = \frac{1}{2m}\left(\vec{p} + \frac{e}{c}\vec{A}_{tot}(t)\right)^2 + V_{ion}(\vec{r},t) + \int d^3\vec{r'}\frac{\rho(\vec{r'},t)}{|\vec{r} - \vec{r'}|} + V_{xc}(\vec{r},t) \quad (4)$$

in which $V_{ion}(\vec{r},t)$ is the electron−ion interaction potential and $V_{xc}(\vec{r},t)$ is the exchange−correlation potential. $\vec{A}_{tot}(t)$ is the time-dependent vector potential, which is given as $\vec{A}_{tot}(t) = \vec{A}_{ex}(t) + \vec{A}_{ind}(t)$, where $\vec{A}_{ex}(t)$ and $\vec{A}_{ind}(t)$ are the external and induced vector potentials, respectively. The external laser field is obtained from a relation $\vec{E}_{Laser}(t) = -d\vec{A}_{ex}(t)/dt$. The third term in the eq 4 is the Hartree term for the interaction between electrons, with time-dependent charge density given by

$$\rho(\vec{r},t) = \sum_i |\psi_i(\vec{r},t)|^2 \quad (5)$$

In this work, we have taken the external electric field as an enveloped wave-train pulse with its corresponding vector potential having the following form,

$$\mathbf{A}_{ex}(t) = \frac{E_0}{\omega}e^{-(t-t_0)^2/2\tau_0^2}\cos(\omega t)\hat{e}_z \quad (6)$$

where E_0 is the amplitude of the time-dependent electric field $E(t)$ with laser carrier frequency ω and of $2\tau_0$ duration. The enveloped wave-train pulse allows reducing the total simulation time as the electric field becomes almost zero at the end of the envelope. The number of excited valence electrons $n_{ex}(t)$ per unit cell is given by

$$n_{ex}(t) = \sum_{nn'k}(\delta_{nn'k} - |\langle\psi_{nk}(0)|\psi_{n'k}(t)\rangle|^2) \quad (7)$$

where n and n' are occupied Kohn−Sham orbital indices, k is a Bloch wave vector, and δ is the Kroneker delta function.

The average induced current density as a function of time $\vec{J}(t)$ is given by[23,43]

$$\vec{J}(t) = -\frac{e}{m_e V}\int_V d\vec{r}\sum_i \mathrm{Re}\psi_i^*(\vec{r},t)\left(\vec{p} + \frac{e}{c}\vec{A}(t)\right)\psi_i(\vec{r},t) + J_{NL}(t) \quad (8)$$

The last term in the above equation comes from the nonlocality of the pseudopotential.

The TDDFT calculations were performed in the real-space, real-time framework as implemented in the Octopus code.[44,45] The interaction between valence electrons and ion cores is described by the Hartwigsen−Goedecker−Hutter pseudopotentials[46] along with the Tran−Blaha (TB09) meta-generalized gradient approximation for the exchange functional. In the time-evolution of Kohn−Sham states, approximated enforced time-reversal symmetry propagators were used. The ions had fixed positions throughout the simulations. The orbital wave functions are represented on a three-dimensional real-space grid, with 0.16 Å spacing. The k-grid employed was 8 × 8 × 1. The total simulation time taken was 1240 atomic units (≈30 fs) with a step of 0.015 a.u.

RESULTS AND DISCUSSION

The applied electric field has different effects on the material depending upon its frequency and intensity. Hence, for comparison, we first studied the linear effect, in which a very low-intensity pulsed laser interacts with phosphorene. In this case, a Gaussian enveloped cosinusoidal pulsed laser is used. The reference pulse has such a low intensity (10^9 W/cm^2) that negligible nonlinear effects are present. Subsequently, strong linearly polarized laser fields with different intensities of the order of 10^{12} W/cm^2 with the wave vectors perpendicular to the phosphorene sheet are applied. The variation of a number of excited valence electrons per unit cell (n_{ex}) in the system with the propagation time of the applied intense linearly polarized laser pulse of 1.16 eV carrier frequency is shown in Figure 2. The population of occupied bands and hence n_{ex} changes in sync with the applied laser field. The reference field is weak enough not to excite any electrons from the valence bands. Even though the laser intensities of the order of 10^{12} W/cm^2 are applied, the n_{ex} reaches its original value at the end of the laser pulse. Hence, no multiphoton absorption is taking place at these intensities.

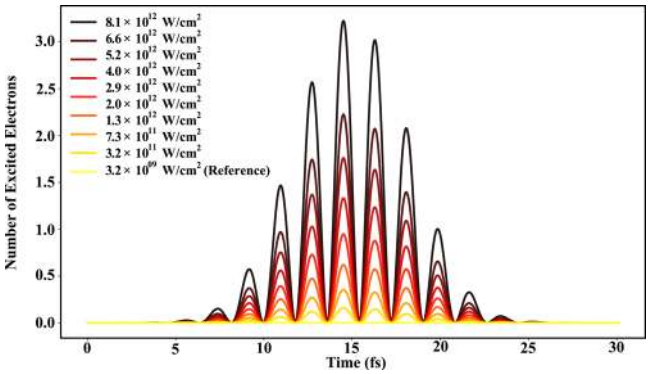

Figure 2. Number of excited valence electrons per unit cell in phosphorene in response to a linearly polarized laser with 1.16 eV carrier frequency and various intensities.

Because of interaction of laser field with the material, the total energy of the system changes with time. Figure 3a,b shows the corresponding changes in the total energy of the unit cell with lasers of various intensities for two laser frequencies. When the laser frequency is less than the band gap (1.19 eV at TB09 level) of the material, the amount of pumped energy increases up to the pulse peak and starts decreasing on the trailing part of the pulse. This is because, with increasing intensity, the laser field does more work to displace excited electrons from their field-free positions. The material regains the original energy value at the end of the pulse, irrespective of the laser intensity employed here. Hence, the energy transfer from the laser field to the material is completely reversible. However, when the laser frequency is set higher than the band gap of the material, the total energy of the system saturates to a value higher than the value it started with. This energy difference can be termed as the irreversible amount of energy W_{irrev} pumped into the system, while the difference between the highest peak and the saturation value gives the reversible energy W_{rev}. As the name suggests, the irreversible energy is lost in the system, and its dissipation can only be tracked if we couple the electronic system with Maxwell's equations. For electronic device applications, apart from other factors, the

DOI: 10.1021/acs.jpcc.8b04134
J. Phys. Chem. C 2018, 122, 19146−19152

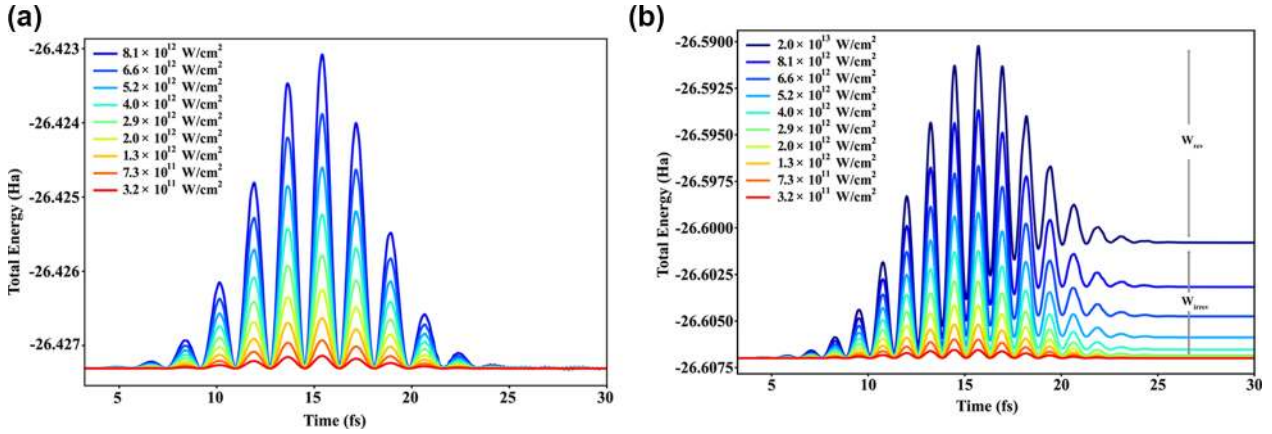

Figure 3. Change in the total energy of phosphorene unit cell induced due to a few-cycle linearly polarized femtosecond laser of (a) 1.16 eV (less than the band gap) and (b) 1.64 eV (greater than the band gap) energy for various intensities. The total energy change varies in synchronization with the leading part of the laser pulse, following the pattern of the population of excited states, but has higher saturation energy values for the laser with energy higher than the band gap of the material. The amount of irreversible energy (W_{irrev}) deposited into the sample is the difference of the total energy at the end of the driving field and at the beginning, while reversible energy (W_{rev}) is the difference between the highest total energy and the saturated total energy at the end of the laser.

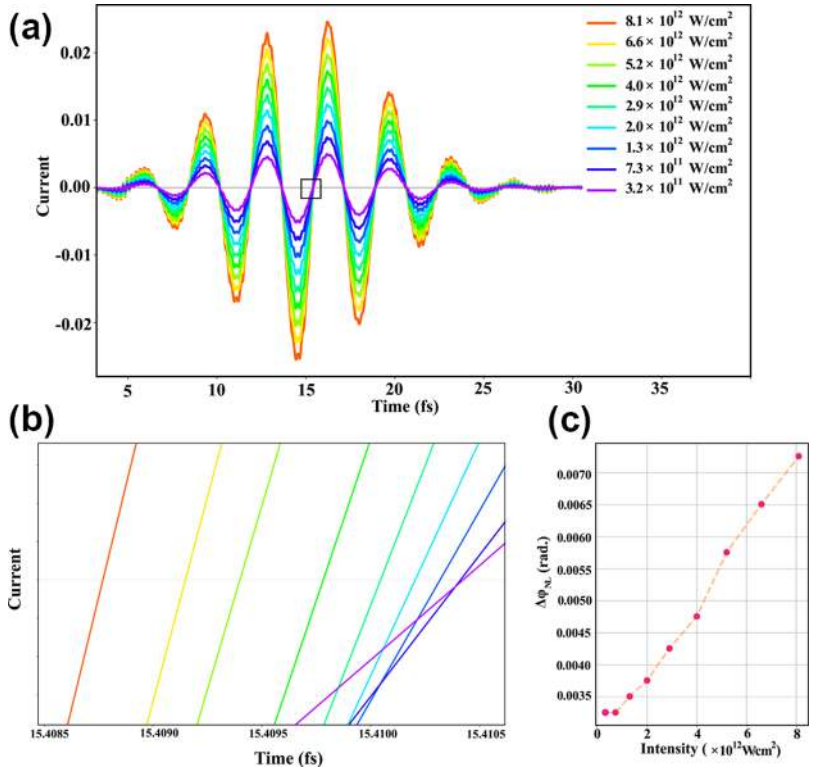

Figure 4. (a) Few-cycle laser pulse with various high intensities induces a microscopic current, which is phase-shifted in comparison to the reference low-intensity laser field as a result of a nonlinear light-matter interaction. A transient positive phase-shift due to a 1.16 eV linearly polarized laser is observed with increasing intensities primarily due to the change in the refractive index of the material as is observed in the optical Kerr effect. (b) Zoomed portion shows maximum shifts regime. (c) Variation of maximum nonlinear phase shift induced due to the linearly polarized laser with 1.16 eV laser frequency for various intensities.

ratio of W_{rev}/W_{irrev} should be as high as possible to limit the amount of heat loss in the system. Some high-frequency oscillations at the end of the pulse (cf. Figure 3a) are due to numerical artifacts.

The electric field of the laser induces the current (cf. eq 8) in the system. The variation of this induced current with time for various intensities of the laser is shown in Figure 4a. The induced current increases with the intensity of the laser field and gradually reaches zero at the end of the laser pulse. However, the induced current is slightly phase-shifted (on sub-femtosecond timescale) compared to the low-intensity reference laser field as shown in Figure 4b. The nonlinear phase shift $\Delta\phi_{NL}(t)$ increases with the applied field amplitude, however gradually saturates. For a given laser intensity, it rises toward the peak of the pulse and vanishes when laser pulse has been switched off. This phase shift is primarily observed because of the transient change in the refractive index because of increased charge carriers induced by the intense laser

DOI: 10.1021/acs.jpcc.8b04134
J. Phys. Chem. C 2018, 122, 19146−19152

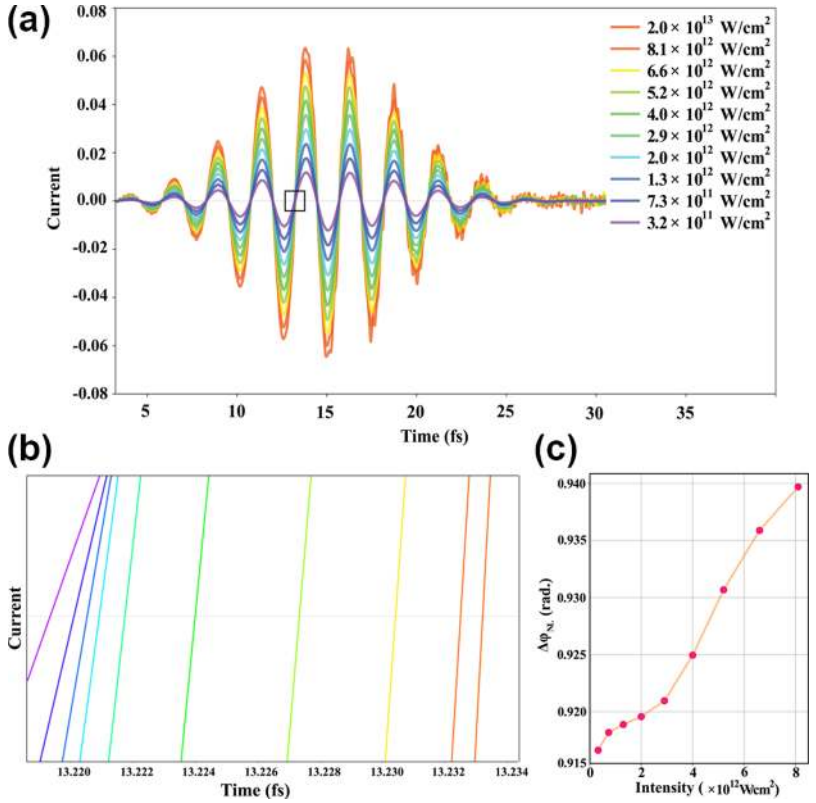

Figure 5. (a) For a few-cycle laser with linear polarization with 1.65 eV carrier frequency, the transient shift in the electric field of the laser due to the change in the refractive index of the material is shown. (b) Zoomed portion displays the maximum shifts regime. (c) Maximum nonlinear phase shift induced due to the linearly polarized laser with 1.65 eV carrier frequency for various intensities.

fields.[40] The nonlinear phase shift varies approximately linearly with the intensity of the linearly polarized laser as shown in Figure 4c, indicating that the field intensities are below the dielectric breakdown thresholds.

For laser fields with the frequency higher than the band gap (i.e., 1.65 eV), the induced currents as well as the nonlinear phase shifts exhibit significant enhancement, as shown in Figure 5a,b. This is expected because the refractive index of the material depends on the light frequency as well as the intensity, so is the change in the above-mentioned phase shift. This shift is still at the sub-femtosecond level. In the case of a higher laser frequency also, the nonlinear phase shift varies linearly with the applied field's intensity, indicating that the laser intensities are within the limit of optical damage threshold. The magnitude of the nonlinear phase shifts are higher compared to the laser frequencies less than the band gap of the material, implying a dominant optical Kerr effect.

The amount of irreversible energy pumped into the system is related to the number of valence electrons excited into the conduction band, given by a relation

$$N_{exc} \approx W_{irrev}/\Delta_g \tag{9}$$

where Δ_g is the band gap of the material and W_{irrev} is the energy dissipated per unit cell.[24] Therefore, for a linearly polarized laser with 1.65 eV frequency has around 0.0065 eV pumped in for 8×10^{12} W/cm^2 field, giving approximately $N_{exc} = 0.0054N_{VB}$, with N_{VB} being the number of valence electrons. This seemingly small amount of carriers, which is detectable with such a precision using this sub-femtosecond spectroscopy, is responsible for changing the dielectric constant of the material, rendering the material to be used as an ultrafast signal processor. The relation between the change in the refractive index of the material and the number of excited electrons is given as

$$\Delta n = -\frac{e^2 n_e}{2\epsilon_0 m_e^* \omega^2 n(\omega)} \tag{10}$$

where ϵ_0 is the vacuum permittivity, n_e is the excited electrons density, ω is the corresponding plasma frequency, and $n(\omega)$ is the frequency-dependent refractive index. The leading edge of the laser field pulse supplies the energy flow into the system and is returned to the driving field on the trailing edge, usually accompanied by a temporal shift in the pulse peak at the sub-femtosecond timescale. This phase shift is a manifestation of reversible energy transfer between the fields and matter.[40] This field-induced change in the phase of the pulse is linked to the change in the refractive index of the material. For the above-mentioned case, the irreversible energy density turns out to be 1.1×10^8 eV/μm^3, to be compared with the 10^9 eV/μm^3 of the state-of-the-art metal−oxide−semiconductor field-effect transistor operating at 9 GHz of current age digital electronics.[24] The speed limiting factors in the CMOS circuits are mainly heat dissipation and gate delays. However, the former becomes a bottleneck much before the latter kicks in. Hence, achieving the on/off operation with as small as possible dissipation gets paramount importance. Achieving such a low dissipation in CMOS circuits with very large scale integration poses many challenges. This is one of the main reasons behind the CPU clock speed remaining stagnant around 4 GHz for a very long time.[47] Our approach may help in devising an entirely different setup of laser assisted electronics, where higher operating frequencies can be easily achieved. The problem of band gap

DOI: 10.1021/acs.jpcc.8b04134
J. Phys. Chem. C 2018, 122, 19146−19152

change by substrating the phosphorene can be circumvented by a suitable choice of laser frequency and higher band gap substrate.

In all these cases, the ultrafast nonlinear spectroscopy enables us to study the complex nature of the dynamical exchange of energy between the matter and laser fields. The TDDFT simulations presented here give direct access to microscopic physical quantities, such as photo-induced currents, energy lost in the system, or current-induced changes in the dielectric properties, which can be experimentally verified. The change in the refractive index of the material Δn is dependent on the W_{rev} while the dissipation during this processing is governed by the W_{irrev}; both being important quantities for efficient signal manipulation for the future generation optoelectronic devices. The induced currents can be switched on and off on the femtosecond timescales, at the expense of a very little dissipation. This is to be contrasted to the case of switching in field effect transistors, where energy is dissipated by electron−hole recombinations, whereas in these optical switching the almost all stored energy is returned to the driving electric field. This fact can be utilized to overcome the current speed limit of information processing in digital electronics.

CONCLUSIONS

To summarize, in our real-time, real-space TDDFT simulation, we study the nonlinear electron dynamics in phosphorene and associate the induced nonlinear phase shift and the changes in the number of free charge carriers with the change in the refractive index. With a careful selection of laser field, the 100 GHz signal processing rate can be achieved with this material. The sub-femtosecond nonlinear polarization exhibited by phosphorene under the intense ultrafast laser fields paves a way toward dielectric optical switching. This spectroscopy enables access to the linear and nonlinear polarization in the matter and provides insight into the dynamics of light−matter interaction with the resolution of electronic timescales. In the observed optical Kerr effect, the transient changes in refractive index are reversible up to a certain threshold, suggesting that the nonlinear properties can be changed or a switch can be turned on or off on the timescale of an optical period, enabling the possibility of operating future phosphorene-based electronic devices at the optical frequencies.

ASSOCIATED CONTENT

Supporting Information

The Supporting Information is available free of charge on the ACS Publications website at DOI: 10.1021/acs.jpcc.8b04134.

Linearly polarized few-cycle laser vector potential with frequency and maximum change observed in the refractive index of phosphorene for various intensities of a linearly polarized laser of 1.64 eV frequency (PDF)

AUTHOR INFORMATION

Corresponding Authors

*E-mail: ravindrals@iisc.ac.in (R.S.).
*E-mail: abhishek@iisc.ac.in (A.K.S.).

ORCID

Ravindra Shinde: 0000-0001-5182-1480
Abhishek Kumar Singh: 0000-0002-7631-6744

Notes

The authors declare no competing financial interest.

ACKNOWLEDGMENTS

R.S. acknowledges Science and Engineering Research Board, DST, India, for a fellowship (PDF/2015/000466). We also acknowledge Materials Research Center and Supercomputer Education and Research Centre, Indian Institute of Science, for providing the computational facilities.

REFERENCES

(1) Cavin, R. K.; Lugli, P.; Zhirnov, V. V. Science and Engineering Beyond Moore's Law. *Proc. IEEE* **2012**, *100*, 1720−1749.
(2) Markov, I. L. Limits on fundamental limits to computation. *Nature* **2014**, *512*, 147−154.
(3) Novoselov, K. S. Electric Field Effect in Atomically Thin Carbon Films. *Science* **2004**, *306*, 666−669.
(4) Geim, A. K.; Novoselov, K. S. The Rise of Graphene. *Nat. Mater.* **2007**, *6*, 183−191.
(5) Vogt, P.; De Padova, P.; Quaresima, C.; Avila, J.; Frantzeskakis, E.; Asensio, M. C.; Resta, A.; Ealet, B.; Le Lay, G. Silicene: Compelling Experimental Evidence for Graphene-like Two-Dimensional Silicon. *Phys. Rev. Lett.* **2012**, *108*, 155501.
(6) Bianco, E.; Butler, S.; Jiang, S.; Restrepo, O. D.; Windl, W.; Goldberger, J. E. Stability and Exfoliation of Germanane: A Germanium Graphane Analogue. *ACS Nano* **2013**, *7*, 4414−4421.
(7) Zhu, F.-f.; Chen, W.-j.; Xu, Y.; Gao, C.-l.; Guan, D.-d.; Liu, C.-h.; Qian, D.; Zhang, S.-C.; Jia, J.-f. Epitaxial Growth of Two-Dimensional Stanene. *Nat. Mater.* **2015**, *14*, 1020−1025.
(8) Brent, J. R.; Savjani, N.; Lewis, E. A.; Haigh, S. J.; Lewis, D. J.; O'Brien, P. Production of Few-Layer Phosphorene by Liquid Exfoliation of Black Phosphorus. *Chem. Commun.* **2014**, *50*, 13338−13341.
(9) Liu, H.; Neal, A. T.; Zhu, Z.; Luo, Z.; Xu, X.; Tománek, D.; Ye, P. D. Phosphorene: An Unexplored 2D Semiconductor with a High Hole Mobility. *ACS Nano* **2014**, *8*, 4033−4041.
(10) Wu, M.; Zeng, X. C. Intrinsic Ferroelasticity and/or Multiferroicity in Two-Dimensional Phosphorene and Phosphorene Analogues. *Nano Lett.* **2016**, *16*, 3236−3241.
(11) Gong, P.-L.; Liu, D.-Y.; Yang, K.-S.; Xiang, Z.-J.; Chen, X.-H.; Zeng, Z.; Shen, S.-Q.; Zou, L.-J. Hydrostatic Pressure-Induced Three-Dimensional Dirac Semimetal in Black Phosphorus. *Phys. Rev. B: Condens. Matter Mater. Phys.* **2016**, *93*, 195434.
(12) Tran, V.; Soklaski, R.; Liang, Y.; Yang, L. Layer-Controlled Band Gap and Anisotropic Excitons in Few-Layer Black Phosphorus. *Phys. Rev. B: Condens. Matter Mater. Phys.* **2014**, *89*, 235319.
(13) Manjanath, A.; Samanta, A.; Pandey, T.; Singh, A. K. Semiconductor to metal transition in bilayer phosphorene under normal compressive strain. *Nanotechnology* **2015**, *26*, 075701.
(14) Li, L.; Kim, J.; Jin, C.; Ye, G. J.; Qiu, D. Y.; da Jornada, F. H.; Shi, Z.; Chen, L.; Zhang, Z.; Yang, F.; et al. Direct Observation of the Layer-Dependent Electronic Structure in Phosphorene. *Nat. Nanotechnol.* **2016**, *12*, 21−25.
(15) Li, L.; Yu, Y.; Ye, G. J.; Ge, Q.; Ou, X.; Wu, H.; Feng, D.; Chen, X. H.; Zhang, Y. Black Phosphorus Field-Effect Transistors. *Nat. Nanotechnol.* **2014**, *9*, 372−377.
(16) Li, D.; Jussila, H.; Karvonen, L.; Ye, G.; Lipsanen, H.; Chen, X.; Sun, Z. Polarization and Thickness Dependent Absorption Properties of Black Phosphorus: New Saturable Absorber for Ultrafast Pulse Generation. *Sci. Rep.* **2015**, *5*, 15899.
(17) Uddin, S.; Debnath, P. C.; Park, K.; Song, Y.-W. Nonlinear Black Phosphorus for Ultrafast Optical Switching. *Sci. Rep.* **2017**, *7*, 43371.
(18) Lu, S. B.; Miao, L. L.; Guo, Z. N.; Qi, X.; Zhao, C. J.; Zhang, H.; Wen, S. C.; Tang, D. Y.; Fan, D. Y. Broadband Nonlinear Optical Response in Multi-Layer Black Phosphorus: An Emerging Infrared and Mid-Infrared Optical Material. *Opt. Express* **2015**, *23*, 11183.

DOI: 10.1021/acs.jpcc.8b04134
J. Phys. Chem. C 2018, 122, 19146−19152

(19) Sun, Z.; Martinez, A.; Wang, F. Optical Modulators with 2D Layered Materials. *Nat. Photonics* **2016**, *10*, 227−238.
(20) Jiang, X.-F.; Zeng, Z.; Li, S.; Guo, Z.; Zhang, H.; Huang, F.; Xu, Q.-H. Tunable Broadband Nonlinear Optical Properties of Black Phosphorus Quantum Dots for Femtosecond Laser Pulses. *Materials* **2017**, *10*, 210.
(21) Sotor, J.; Sobon, G.; Macherzynski, W.; Paletko, P.; Abramski, K. M. Black Phosphorus Saturable Absorber for Ultrashort Pulse Generation. *Appl. Phys. Lett.* **2015**, *107*, 051108.
(22) Zheng, J.; Tang, X.; Yang, Z.; Liang, Z.; Chen, Y.; Wang, K.; Song, Y.; Zhang, Y.; Ji, J.; Liu, Y.; et al. Few-Layer Phosphorene-Decorated Microfiber for All-Optical Thresholding and Optical Modulation. *Adv. Opt. Mater.* **2017**, *5*, 1700026.
(23) *Fundamentals of Time-Dependent Density Functional Theory*; Marques, M. A. L., Maitra, N. T., Nogueira, F. M., Gross, E., Rubio, A., Eds.; Springer Berlin Heidelberg, 2012.
(24) Sommer, A.; Bothschafter, E. M.; Sato, S. A.; Jakubeit, C.; Latka, T.; Razskazovskaya, O.; Fattahi, H.; Jobst, M.; Schweinberger, W.; Shirvanyan, V.; et al. Attosecond nonlinear polarization and light-matter energy transfer in solids. *Nature* **2016**, *534*, 86−90.
(25) Yabana, K.; Sugiyama, T.; Shinohara, Y.; Otobe, T.; Bertsch, G. F. Time-Dependent Density Functional Theory for Strong Electromagnetic Fields in Crystalline Solids. *Phys. Rev. B: Condens. Matter Mater. Phys.* **2012**, *85*, 045134.
(26) Jiao, Y. L.; Wang, F.; Hong, X. H.; Su, W. Y.; Chen, Q. H.; Zhang, F. S. Electron dynamics in CaB6 induced by one- and two-color femtosecond laser. *Phys. Lett. A* **2013**, *377*, 823−827.
(27) Gao, L. L.; Wang, F.; Jiang, L.; Qu, L. T.; Lu, Y. F. Optical-induced electrical current in diamond switched by femtosecond-attosecond laser pulses byab initiosimulations. *J. Phys. D: Appl. Phys.* **2015**, *49*, 025102.
(28) Su, G.; Jiang, L.; Wang, F.; Qu, L.; Lu, Y. First-Principles Simulations for Excitation of Currents in Linear Carbon Chains under Femtosecond Laser Pulse Irradiation. *Phys. Lett. A* **2016**, *380*, 2453−2457.
(29) Schlaepfer, F.; Lucchini, M.; Sato, S. A.; Volkov, M.; Kasmi, L.; Hartmann, N.; Rubio, A.; Gallmann, L.; Keller, U. Attosecond optical-field-enhanced carrier injection into the GaAs conduction band. *Nat. Phys.* **2018**, *14*, 560−564.
(30) Schultze, M.; Bothschafter, E. M.; Sommer, A.; Holzner, S.; Schweinberger, W.; Fiess, M.; Hofstetter, M.; Kienberger, R.; Apalkov, V.; Yakovlev, V. S.; et al. Controlling Dielectrics with the Electric Field of Light. *Nature* **2012**, *493*, 75−78.
(31) Garg, M.; Zhan, M.; Luu, T. T.; Lakhotia, H.; Klostermann, T.; Guggenmos, A.; Goulielmakis, E. Multi-Petahertz Electronic Metrology. *Nature* **2016**, *538*, 359−363.
(32) Otobe, T.; Shinohara, Y.; Sato, S. A.; Yabana, K. Femtosecond Time-Resolved Dynamical Franz-Keldysh Effect. *Phys. Rev. B: Condens. Matter Mater. Phys.* **2016**, *93*, 045124.
(33) Schiffrin, A.; Paasch-Colberg, T.; Karpowicz, N.; Apalkov, V.; Gerster, D.; Mühlbrandt, S.; Korbman, M.; Reichert, J.; Schultze, M.; Holzner, S.; et al. Optical-Field-Induced Current in Dielectrics. *Nature* **2012**, *493*, 70−74.
(34) Krausz, F.; Ivanov, M. Attosecond Physics. *Rev. Mod. Phys.* **2009**, *81*, 163−234.
(35) Wachter, G.; Lemell, C.; Burgdörfer, J.; Sato, S. A.; Tong, X.-M.; Yabana, K. Ab Initio Simulation of Electrical Currents Induced by Ultrafast Laser Excitation of Dielectric Materials. *Phys. Rev. Lett.* **2014**, *113*, 087401.
(36) Suess, R. J.; Leong, E.; Garrett, J. L.; Zhou, T.; Salem, R.; Munday, J. N.; Murphy, T. E.; Mittendorff, M. Mid-Infrared Time-Resolved Photoconduction in Black Phosphorus. *2D Mater.* **2016**, *3*, 041006.
(37) Wang, K.; Szydłowska, B. M.; Wang, G.; Zhang, X.; Wang, J. J.; Magan, J. J.; Zhang, L.; Coleman, J. N.; Wang, J.; Blau, W. J. Ultrafast Nonlinear Excitation Dynamics of Black Phosphorus Nanosheets from Visible to Mid-Infrared. *ACS Nano* **2016**, *10*, 6923−6932.
(38) Su, G.; Wang, F.; Jiang, L.; Zhang, X.; Su, X.; Qu, L.; Lu, Y. Ultrafast Response of Dielectric Properties of Monolayer Phosphorene to Femtosecond Laser. *J. Appl. Phys.* **2017**, *121*, 173105.
(39) Boyd, R. *Nonlinear Optics*; Academic Press, 2008.
(40) Wegener, M. *Extreme Nonlinear Optics*; Springer-Verlag Berlin, 2005.
(41) Krause, J. L.; Schafer, K. J.; Kulander, K. C. Calculation of photoemission from atoms subject to intense laser fields. *Phys. Rev. A* **1992**, *45*, 4998−5010.
(42) *Digital Integrated Circuits: A Design Perspectives*; Rabaey, J. M., Chandrasekaran, A., Nikolic, B., Eds.; Pearson Education, 2003.
(43) *Time-Dependent Density Functional Theory*; Marques, M. A., Ullrich, C. A., Nogueira, F., Rubio, A., Burke, K., Gross, E. K. U., Eds.; Springer Berlin Heidelberg, 2006.
(44) Castro, A.; Appel, H.; Oliveira, M.; Rozzi, C. A.; Andrade, X.; Lorenzen, F.; Marques, M. A. L.; Gross, E. K. U.; Rubio, A. octopus: A Tool for the Application of Time-Dependent Density Functional Theory. *Phys. Status Solidi B* **2006**, *243*, 2465−2488.
(45) Andrade, X.; Strubbe, D.; De Giovannini, U.; Larsen, A. H.; Oliveira, M. J. T.; Alberdi-Rodriguez, J.; Varas, A.; Theophilou, I.; Helbig, N.; Verstraete, M. J.; et al. Real-Space Grids and the Octopus Code as Tools for the Development of New Simulation Approaches for Electronic Systems. *Phys. Chem. Chem. Phys.* **2015**, *17*, 31371−31396.
(46) Hartwigsen, C.; Goedecker, S.; Hutter, J. Relativistic Separable Dual-Space Gaussian Pseudopotentials from H to Rn. *Phys. Rev. B* **1998**, *58*, 3641−3662.
(47) Why has CPU frequency ceased to grow? https://software.intel.com/en-us/blogs/2014/02/19/why-has-cpu-frequency-ceased-to-grow; Intel Software Developer Zone, article published in 2014.

DOI: 10.1021/acs.jpcc.8b04134
J. Phys. Chem. C 2018, 122, 19146−19152